AD-A101 620    LAMONT-DOHERTY GEOLOGICAL OBSERVATORY PALISADES NY        F/G 8/3
                ARCTIC OCEAN EDDIES AND BAROCLINIC INSTABILITY.(U)
                JUL 81  K HUNKINS                                        N00014-76-C-0004
UNCLASSIFIED    LDGO-CU-2-81                                             NL

1 OF 1
AD A
A101 620

END
DATE
FILMED
8-81
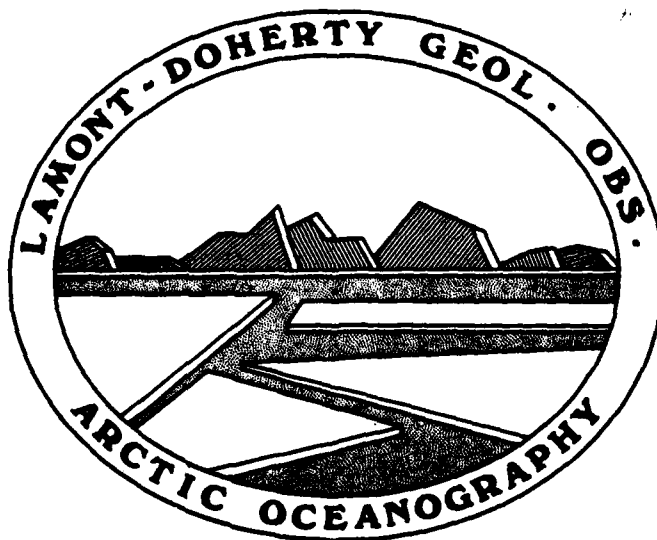DTIC

LEVEL

# ARCTIC OCEAN EDDIES AND

# BAROCLINIC INSTABILITY

AD A101620

by Kenneth Hunkins

# CU-2-81 TECHNICAL REPORT No. 2

DTIC
ELECTE
JUL 1 7 1981
C



LAMONT-DOHERTY GEOL. OBS.
ARCTIC OCEANOGRAPHY

81 7 16 079

DTIC FILE COPY

# ARCTIC OCEAN EDDIES AND

# BAROCLINIC INSTABILITY

by Kenneth Hunkins

# CU-2-81  TECHNICAL  REPORT  No. 2

DTIC

JUL 1 7 1981

July 1981

LAMONT-DOHERTY GEOL. OBS.

ARCTIC OCEANOGRAPHY

CU-2-81


ARCTIC OCEAN EDDIES AND
BAROCLINIC INSTABILITY


by


Kenneth Hunkins


LAMONT-DOHERTY GEOLOGICAL OBSEVATORY
of Columbia University
Palisades, N. Y.   10964


July 1981

Accession For
NTIS  GRA&I
DTIC TAB
Unannounced
Justification

By
Distribution/
Availability Codes
Dist     Avail and/or
         Special

A

## ABSTRACT

Baroclinic eddies with diameters of about 10 km and maximum current speeds of about 50 cm/s have been widely observed in the central Arctic Ocean north of Alaska and Canada. The possible origin of these eddies through an instability of the mean baroclinic flow is investigated using an ocean model with exponential profiles of mean shear and Väisälä frequency. The model includes Ekman pumping at a rigid bottom and at either a free or rigid upper surface. The central Arctic Ocean where the eddies were found is baroclinically stable with no possibility of eddy production. If the eddies are spawned by this mechanism, they must be formed at a site far from where they were observed. On the periphery of the Arctic Ocean north of Alaska the combination of greater current shear, shallower depth and lack of ice cover leads to unstable conditions and the eddies apparently originate in that region. The instability theory predicts maximum velocity at the surface instead of below the surface as observed. Apparently after formation in open water the eddies are advected beneath the ice cover and dissipate the momentum of their upper layers against the ice. This is demonstrated by calculations for the diffusion of vorticity against the ice in the case of an initial exponential profile. A subsurface maximum then develops which resembles the observed profiles.

## 1. Introduction.

The temperature, salinity and velocity fields of the oceans have a mesoscale variability on scales of tens to hundreds of kilometers horizontally and on the order of months in time. These mesoscale features frequently take the form of approximately circular baroclinic eddies with a nearly geostrophic force balance. It is likely that mesoscale currents play an important part in driving the large-scale ocean circulation and in transporting heat as well as chemical and biological parameters on a global scale. A review of the literature of mesoscale currents (McWilliams, 1979) shows that these features have been widely observed and appear to be nearly ubiquitous in the world ocean.

Mesoscale eddies in the Arctic Ocean were reported by Hunkins (1974) and Newton et al (1974) based on research carried out from drifting ice stations. During the AIDJEX (Arctic Ice Dynamics Joint Experiment) project in 1975 and 1976, a much more extensive survey was made and large numbers of arctic mesoscale eddies were identified (Hunkins, 1980; Manley, 1981). Profiles of temperature, salinity and current were made on a daily basis from four manned AIDJEX ice camps spaced 100 km apart drifting in the central Arctic Ocean. The arctic eddies are strongly baroclinic with a subsurface velocity maximum in the steep density gradient between 30 and 200 m. Vertical profiles of oceanographic parameters through an arctic eddy and in adjacent waters outside the eddy are shown in Figs. 1 and 2. The maximum current speed of 58 cm/s in this particular eddy contrasts with the geostrophic mean currents in this region which are only 5 to 10 cm/s. During their 14-month drift which covered a total track length of 8,140 km, the four AIDJEX camps encountered 143 eddies. The location of these eddies is shown in Fig. 3.

1

One of the eddies was recrossed after 5½ months, demonstrating that they persist for at least that length of time. There is a peak in mean vertical kinetic energy profiles at 120 m coinciding with the velocity maximum. The kinetic energy of the central Arctic Ocean resides almost entirely in the eddies with the mean currents accounting for less than one per cent. Although detailed surveys of individual eddies are lacking, most of them seem to have a diameter of about 10 km. On that basis, it is estimated that eddies cover between 10 and 20 per cent of the area of the western Arctic Ocean. Their sense of rotation is anticyclonic or clockwise. Water properties within the arctic eddies differ from those without and suggest that these features originate in the shallow waters of the Chukchi Sea.

A number of possible generating mechanisms for these eddies have been suggested including the stress of wind and drifting ice, brine convection accompanying sea ice growth, and an instability of the mean baroclinic current. Of these, the baroclinic instability hypothesis seems most plausible and is the only one examined here in detail.

It is generally accepted that the migrating cyclonic systems of the atmosphere as well as the turbulent flow in certain laboratory experiments with rotating fluids result from the instability to small disturbances of the mean stratified shear flow. This identification of baroclinic instability as a mechanism for generating eddies in the atmosphere and laboratory has produced a body of theory which has been summarized and reviewed by Charney (1973) and Kuo (1973). It has also been suggested that mesoscale eddies observed in the ocean may be initiated by the same instability

mechanism (Orlanski and Cox, 1973; Gill et al, 1974).

One of the simplest theoretical demonstrations of baroclinic instability is that by Eady (1949) who showed that for a basic state in which the vertical shear, Väisälä frequency and Coriolis parameter are all constant, certain intermediate wavelengths are unstable and tend to grow. Since vertical shear and Väisälä frequency are not actually constant in the ocean, models with more realistic structure are desirable for comparison with data. Eady's theory was generalized by Williams (1974) to include mean vertical profiles which vary according to a power law. He further included frictional effects by introducing Ekman pumping at rigid upper and lower boundaries (Williams and Robinson, 1974). The results were successfully applied to interpret rotating tank experiments. For both Eady's and Williams' problems, solutions are in terms of hyperbolic functions.

In the present paper Eady's problem is extended to include mean shear and Väisälä frequency which vary exponentially with depth. Analytical solutions to the problem are in the form of modified Bessel functions. Friction is included in the form of Ekman pumping at either rigid or free surfaces. A model similar to that developed in this paper has been described by Hart and Killworth (1976) who also applied their results to the Arctic Ocean. The model used here differs by including free-surface Ekman pumping and a discussion of vertical wave structure.

Observed eddies in the Atlantic Ocean are in the neighborhood of 200 km in diameter and apparently have their amplitude maximum at the surface. The arctic eddies are only about 10 km in diameter and have their maximum amplitude in the pycnocline well below the

3

surface. These differences between eddies in the Atlantic and
Arctic Oceans suggested an investigation of factors influencing the
horizontal scale and vertical profile of the disturbance. The
shape of the mean shear and stability profiles as well as the pres-
ence of the ice cover on the Arctic Ocean are expected to be impor-
tant factors.

## 2. The Exponential Eady Problem.

The analysis is based on the quasi-geostrophic potential vor-
ticity equation in a form used extensively in oceanography and
meteorology. For an ocean with a mean state varying only with
depth and which is disturbed by small perturbations in pressure and
density we have

$$p = p_0(z) + p'(x, y, z, t)$$

and

$$\rho = \rho_0(z) + \rho'(x, y, z, t)$$

where the perturbations, p' and $\rho'$, are much smaller than the mean
values. If there is a geostrophic balance so that

$$u = -\frac{1}{\rho_0 f} \frac{\partial p'}{\partial y} = -\frac{\partial \psi}{\partial y}$$

and

$$v = \frac{1}{\rho_0 f} \frac{\partial p'}{\partial x} = \frac{\partial \psi}{\partial x}$$

where $\psi = p'/\rho_0 f$ is the geostrophic stream function,

4

then the quasi-geostrophic equation may be written

$$\frac{D}{Dt}\left\{\nabla^2\psi + \frac{\partial}{\partial z}\left(\frac{f^2}{N^2}\frac{\partial\psi}{\partial z}\right)\right\} + \beta\frac{\partial\psi}{\partial x} = 0$$

(2.1)

where directions are x, east; y, north; z, vertically upward; and the north and east velocity components are u and v. The Coriolis parameter, f, has its usual meaning. Other symbols are defined as follows:

Total derivative, $\quad \dfrac{D}{Dt} = \dfrac{\partial}{\partial t} + u\dfrac{\partial}{\partial x} + v\dfrac{\partial}{\partial y}$

Horizontal Laplacian, $\quad \nabla^2 = \dfrac{\partial^2}{\partial x^2} + \dfrac{\partial^2}{\partial y^2}$

Väisälä frequency, $\quad N^2 = -\dfrac{g}{\rho_0}\dfrac{\partial\rho_0}{\partial z}$

Beta parameter, $\quad \beta = \dfrac{\partial f}{\partial y}$

The quantity in brackets is the potential vorticity, composed of the relative vorticity and the stretching effect of density gradients on vortex lines. The final term of the equation represents the effect of meridional motions on potential vorticity. For the derivation of this equation and discussion, see Pedlosky (1979).

Assuming a stream function composed of steady and perturbation parts

$$\psi = -y\,U(z) + \varphi(x, y, z, t)$$

where the steady eastward flow varies only with depth, the linearized form of (2.1) becomes

$$\left(\frac{\partial}{\partial t} + U\frac{\partial}{\partial x}\right)\left\{\nabla^2\varphi + \frac{\partial}{\partial z}\left(\frac{f^2}{N^2}\frac{\partial\varphi}{\partial z}\right)\right\} - \frac{\partial\varphi}{\partial x}\frac{\partial}{\partial z}\left(\frac{f^2}{N^2}\frac{\partial U}{\partial z}\right) + \beta\frac{\partial\varphi}{\partial x} = 0$$

(2.2)

This equation may be separated by introducing a perturbation stream function in the form of a zonally-propagating wave,

$$\varphi = R_e \ F(z) \ \sin \ my \ e^{ik(x-ct)}$$

to give the differential equation for vertical structure

$$(U - c)\left\{\frac{d}{dz}\left(\frac{f^2}{N^2}\frac{dF}{dz}\right) - \left(k^2 + m^2\right)F\right\} + \left\{\beta - \frac{d}{dz}\left(\frac{f^2}{N^2}\frac{dU}{dz}\right)\right\}F = 0$$

(2.3)

If both $N^2$ and $dU/dz$ have the same functional form and $\beta = 0$, the final term in brackets vanishes and the singularity at $U = c$ is circumvented. This has been called the generalized Eady problem by Williams (1974) who used a power-law dependence for $N^2$ and $dU/dz$. Here we introduce an exponential depth dependence for those quantities.

Let the basic density variation take an exponential form

$$\rho_o(z) = \rho_s + \Delta\rho\left(1 - e^{\alpha z}\right)$$

where $\rho_s$ is the density value at the surface and $\Delta\rho$ is the difference in density between the surface and great depths.

The Väisälä frequency in this case becomes,

$$N^2 = \frac{g \, \alpha \, \Delta\rho \, e^{\alpha z}}{\rho_s + \Delta\rho(1 - e^{\alpha z})} \cong \frac{g \alpha \Delta\rho}{\rho_s} e^{\alpha z}$$

to a good degree of approximation since, for the ocean,

$$\rho_s \cong 10^3 \, kg \cdot m^{-3} \quad , \quad \Delta\rho \cong 1 \, kg \cdot m^{-3}$$

and the scale depth of the pycnocline,

$$\alpha \cong 10^{-3} \, m^{-1}$$

The value of the Väisälä frequency at the surface is

$$N_s^2 = \frac{g \, \alpha \, \Delta\rho}{\rho_s}$$

so that

$$N^2 = N_s^2 \, e^{\alpha z}$$

The basic current takes the same exponential form,

$$U = U_s \, e^{\alpha z}$$

These profiles have a resemblance to those in many regions of the ocean including the Arctic. It can be shown that the association of exponential stratification and exponential shear implies isopycnal surfaces which slope uniformly. Note that for these mean conditions the Richardson number increases exponentially with depth,

$$R_i = \left(\frac{N}{dU/dz}\right)^2 = \left(\frac{N_s}{\alpha U_s}\right)^2 e^{-\alpha z}$$

7

Introducing these exponential mean conditions into (2.3) produces the non-dimensional differential equation,

$$\frac{d^2 F}{dz^2} - \frac{dF}{dz} - e^{\hat{z}} \hat{\gamma}^2 F = 0$$

(2.4)

Circumflexes indicate parameters which have been scaled by the depth of the pycnocline, $\hat{z} = \alpha z$, and by an internal Rossby radius of deformation,

$$\hat{k} = \frac{N_s}{\alpha f} k \quad , \quad \hat{m} = \frac{N_s}{\alpha f} m$$

and

$$\hat{\gamma} = \left( \hat{k}^2 + \hat{m}^2 \right)^{1/2}$$

Introduction of a change of variable,

$$F(z) = p \, P(p)$$

where

$$p = 2 \hat{\gamma} e^{\hat{z}/2}$$

transforms (2.4) into a standard form of the Bessel equation,

$$\frac{d^2 P}{dp^2} + \frac{1}{p} \frac{dP}{dp} - \left( 1 + \frac{1}{p^2} \right) P = 0$$

(2.5)

which has a solution in terms of modified Bessel functions of the first order,

$$P = A \, I_1(p) + B \, K_1(p)$$

8

where A and B are arbitrary constants. Returning to the original dependent variable, the solution becomes

$$F(\varphi) = A \, p \, I_1(\varphi) + B \, p \, K_1(\varphi)$$

(2.6)

Boundary conditions at the surface and bottom are imposed by Ekman pumping as introduced by Charney and Eliassen (1949). Vorticity of the interior frictionless flow leads to horizontal mass divergence in the Ekman boundary layer and consequent vertical flow at the interface between the interior and the boundary layer. Thus frictional effects in the boundary layers are communicated to the interior as vertical velocities. The Ekman pumping boundary conditions imposed on the vertical velocity,

$$\omega = -\frac{f}{N^2} \frac{D}{Dt}\left(\frac{\partial \psi}{\partial z}\right)$$

$$= -i k \frac{f}{N^2}\left\{(U-c)\frac{\partial \varphi}{\partial z} - \frac{\partial U}{\partial z}\varphi\right\}$$

are either

$$\omega_u = -\frac{D_e}{2}\zeta_g \qquad \text{for a rigid upper surface, such as an ice cover}$$

(2.7)

or

$$\omega_u = -\frac{D_e^2}{2}\frac{\partial \zeta_g}{\partial z} \qquad \text{for a stress-free upper surface as in the case of an open ocean}$$

(2.8)

For a lower rigid surface the Ekman pumping condition is

$$w_L = D_e \, \zeta_g / 2$$

The geostrophic vorticity is defined as

$$\zeta_g = \nabla^2 \varphi = -(k^2 + m^2)\varphi$$

The scale depth of the frictional boundary layer is

$$D_e = (2\nu/f)^{1/2}$$

where $\nu$ is a kinematic eddy viscosity.

Substitution of (2.6) into the boundary conditions gives two equations in terms of the two unknown amplitudes, A and B. For rigid upper and lower boundaries, the equations are

$$A\left[(1-\hat{c})\hat{\gamma} I_0(p_0) - I_1(p_0) - i Y \hat{\gamma} I_1(p_0)\right]$$

$$+ B\left[(\hat{c}-1)\hat{\gamma} K_0(p_0) - K_1(p_0) - i Y \hat{\gamma} K_1(p_0)\right] = 0$$

$$(2.9)$$

and

$$A\left[(e^{-\hat{H}} - \hat{c})\hat{\gamma} I_0(p_H) - e^{-\hat{H}/2} I_1(p_H) + i Y \hat{\gamma} e^{-\hat{H}/2} I_1(p_H)\right]$$

$$+ B\left[(\hat{c}-e^{-\hat{H}})\hat{\gamma} K_0(p_H) - e^{-\hat{H}/2} K_1(p_H) + i Y \hat{\gamma} e^{-\hat{H}/2} K_1(p_H)\right] =$$

$$(2.10)$$

where $\quad p_0 = 2\hat{\gamma} \quad$ and $\quad p_H = 2\hat{\gamma} e^{-\hat{H}/2}$

while for a free upper surface (2.9) is replaced by

$$A\left[(1-\hat{c})\,\hat{\gamma}\,I_0(p_0) - I_1(p_0) - iW\hat{\delta}^2 I_0(p_0)\right]$$

$$+ B\left[(\hat{c}-1)\,\hat{\gamma}\,K_0(p_0) - K_1(p_0) + iW\hat{\delta}^2 K_0(p_0)\right] = 0 \qquad (2.11)$$

where $\hat{H}$ is the dimensionless ocean depth, $\alpha H$ , and the dimension-less phase velocity is defined by $\hat{c} = c/U_0$. The Ekman pumping parameters are

$$\gamma = D_e N_s / 2U_s \qquad \text{for a rigid surface}$$

and

$$W = D_e^2 \alpha N_s / 2U_s \qquad \text{for a free surface.}$$

For other than trivial solutions, the determinant of the co-efficients, A and B, must vanish. This provides a dispersion equa-tion relating $\hat{c}$ and $\hat{\gamma}$. For real values of $\hat{\gamma}$, $\hat{c}$ is generally complex with the real part, $\hat{c}_r$, representing the phase speed and the imagi-nary part, $\hat{c}_i$, representing the growth or decay of the wave. Positive values of $\hat{c}_i$ indicate growing waves or instability. In this case the dispersion equation is a quadratic with two roots and the solutions consist of either a pair of neutral waves, both with $\hat{c}_i = 0$, or one growing and one decaying wave. The roots, calculated with the aid of a digital computer, are plotted in Fig. 4 for $\hat{H} = 5$ and in Fig. 5 for $\hat{H} = 10$. Three types of boundary conditions were used: frictionless, free-rigid and rigid-rigid. The phase speeds, $\hat{c}_r$, are plotted for both the growing and decaying waves. Note that for free-rigid boundary conditions the lower left-hand branch of

11

the phase speed curve is associated with growing waves while for the rigid-rigid case it is the upper branch which corresponds to growing waves. The growth rate, $\hat{\gamma}c_i$, is plotted only for the growing waves. The examples all show a maximum growth rate at some intermediate wave number and a critical wave number beyond which no growth takes place. These results are qualitatively similar to results by others for Eady-type models. When the wave is unchanging in the y-direction, $\hat{m} = 0$ and $\hat{\gamma} = \hat{k}$ to give the highest values of the wave number for the growth maximum and for the critical point beyond which growth ceases. The scaled water depth in Fig. 4, $\hat{H} = 5$, corresponds generally with mid-ocean conditions where the scale depth of the pycnocline is about 1 km and the total water depth about 5 km.

The highest growth rate is found for the case with no Ekman pumping where $\hat{\gamma}\hat{c}_i = 0.134$ at a wave number of 0.8 when $\hat{H} = 5$. Beyond the critical wave number, $\hat{\gamma} = 1.18$, no growth occurs and only neutral waves exist. When Ekman pumping is introduced the growth rate is reduced and the wave numbers of the maximum and critical points are shifted to lower values. For values of $Y = 0.5$ and $W = 0.05$, chosen to correspond roughly to oceanic conditions, the dimensionless growth rate is reduced to 0.068 for a free upper surface and to 0.02 for a rigid upper surface, with rigid bottom surfaces in both cases. For a larger ratio of pycnocline depth to total depth, $\hat{H} = 10$, growth rates as well as phase speeds are less (Fig. 5).

The phase speeds of the decaying and growing waves coincide in the frictionless case, while the phase speeds of the neutral waves split into two separate branches. The presence of Ekman layers

splits the phase speeds for the growing and decaying waves also into
two separate branches.

Vertical profiles for the fastest growing wave are shown in
Figs. 6, 7 and 8 for three different boundary conditions. The rela-
tive perturbation stream function may be represented as

$$\phi/A = R_e \left[ A'(z) + i B'(z) \right] \left[ \cos k(x-ct) + i \sin k(x-ct) \right]$$

where the depth function, F, has been decomposed into real and
imaginary parts. The relative magnitude and phase of the perturba-
tion velocity are given by

$$M = \left( A'^2 + B'^2 \right)^{1/2}$$

and

$$\theta = \tan^{-1} \left( B'/A' \right)$$

The perturbation velocity at the upper surface is greater than
that on the lower surface in all of these cases, although in Eady's
original problem the velocity profile was symmetrical about the
middle level. The solutions are monotonic functions of depth in
both problems and there are no maxima at intermediate depths either
with or without Ekman layers.

The negative phase which is plotted in the figures presents a
lateral view of wave tilt in an east-west direction. The backward
tilt of growing waves as the surface is approached is characteristic
of unstable baroclinic waves.

Linear perturbation theory predicts conditions only at the on-
set of instability and does not describe later developments which
occur as the unstable waves continue to amplify. However, it is

13

expected that the wave which initially grows fastest will continue to dominate the spectrum of unstable waves and that it will maintain the general character of its original profile.

The theory presented here does not include the beta-effect as an approximation to the latitudinal variation of the Coriolis parameter. This neglect seems justifiable in the present study since it has been shown by Green (1960) in numerical investigations that although the inclusion of a finite beta-parameter in the Eady problem produces an additional weaker instability maximum at low wave numbers and also destabilizes the high wave numbers, it does not significantly alter either the wave number or the growth rate of the fastest-growing wave which remains essentially the same as in Eady's problem.

## 3. Application to the Arctic Ocean.

First we examine the possibility that the arctic eddies are generated in offshore locations near where they are observed. Examples of profiles for geostrophic current and Väisälä frequency plotted in Figs. 9 and 10 show that an exponential curve roughly fits conditions in the central Arctic Ocean. Appropriate constants based on these data are:

$$N_s = 2 \times 10^{-2} \; s^{-1} \quad , \quad U_s = 2 \times 10^{-2} \; m \cdot s^{-1}$$

$$D_e = 10 \; m \quad , \quad \alpha = 5 \times 10^{-3} \; m^{-1}, \quad H = 2,000 \; m$$

$$f = 1.4 \times 10^{-4} \; s^{-1}$$

The Ekman pumping parameters are then

$$Y = 5 \qquad \text{and} \qquad W = 0.25$$

The exponential model is stable for Y > 1.5 in the case of a rigid top representing the permanent ice cover for $\hat{H} = 10$. Hence the central Arctic Ocean is stable to small disturbances and the eddies cannot originate there by this process. If we choose an improbably low value for the Ekman pumping parameter of Y = 0.5, the flow is unstable but the growth rate

$$\gamma c_i = \left( U_s \propto f / N_s \right) \hat{\gamma} c_i = 1.98 \times 10^{-8} \, s^{-1}$$

corresponding to an e-folding time of 612 days, is much too long for significant growth in this situation. The half wavelength for the fastest-growing wave in this case would be

$$\lambda / 2 = \left( \pi / \hat{\gamma} \right) \left( N_s / \propto f \right) = 256 \, km$$

which is an order of magnitude larger than the observed diameter.

If the arctic eddies are formed in the Arctic Ocean by baroclinic instability, they must originate at some other location where conditions are less stable. At the edge of the Alaskan Continental shelf, higher mean shear, shallower depth and lack of ice cover during late summer all enhance instability. An oceanographic section made by the USS Staten Island in September 1959 across the Alaskan shelf north of Point Barrow (U. S. Naval Oceanographic Office, 1963) provided guidance in selecting parameters for this region: $N_s = 10^{-2} s^{-1}$, $U_s = 10^{-1} m \cdot s^{-1}$, $D_e = 10m$, $\alpha = 10^{-2} m^{-1}$, $H = 1,000m$ (Y = 0.5 and W = 0.05). For free upper and rigid lower boundries, the flow is unstable with a scaled maximum growth rate 0f 0.055 at a scaled wave number of 0.6 corresponding to a dimen-

sional growth rate of 15 days with a half wavelenght of 37 km.
This rapid growth rate indicates that mesoscale eddies should form
in this area. The dimensions of the predicted growing disturbance
are roughly comparable to observed eddy diameters. Eddies thus
formed would be advected by large-scale currents to the sites
where they were observed in the deep ocean away from shelf areas.

On the other side of the Arctic Ocean in the area northwest of
Svalbard there is another region of strong shear which can also be
examined for instability. Warm water from the Atlantic flows north-
ward into the Arctic Ocean on the eastern side of the strait be-
tween Greenland and Svalbard while cold arctic surface water leaves
on the western side. Values for the critical parameters in that
area may be assigned on the basis of a survey by Newton (1977):
$N_s = 10^{-2}s^{-1}$, $U_s = 0.065m \cdot s^{-1}$, $D_e = 7m$, $\alpha = 1.25 \times 10^{-2}m^{-1}$ and
$H = 800m$ so that $y = 0.5$ and $w = 0.05$. The flow is unstable with an
e-folding time of 18 days for the fastest growing half wavelength
of 30 km. These results are similar to those in the Alaskan shelf
region but it is not likely that the observed eddies originate so
far away. Oceanographic surveys are being planned in the eastern
Arctic Ocean which should provide information on eddy population
north of Greenland and Svalbard. Eddies there would be involved in
the exchange of heat and salt between the Atlantic and Arctic Oceans
and may be a factor in climatic change.

4.  Vorticity diffusion and the subsurface current.

Current speeds in the disturbances generated by baroclinic in-
stability have their maximum at the top pf the model which corres-
ponds to the base of the Ekman layer at a depth of about 10 m. Some

explanation is required for the fact that the observed velocity maximum is much deeper, averaging 120 m. If the eddies are indeed generated along the edge of the Alaskan shelf during summer when open water prevails there, then the current maximum will be near the surface at the base of the Ekman layer. If these eddies are then carried by large-scale currents into the central ice-covered ocean, the high surface velocities will decrease rapidly through friction against the ice leaving a subsurface maximum. This hypothesis can be considered quantitatively as a problem of upward vorticity diffusion from an eddy into a surface layer maintained at zero vorticity.

First we need to examine the relation between the Ekman layer and the mixed layer which extends downward to a depth of about 50 m. The mixed layer, which is maintained throughout most of the year by brine convection resulting from ice formation, will be spun down rapidly through friction against the overlying ice cover. Secondary circulations will cause an efficient Ekman spindown of the entire layer on a time scale of

$$\tau_e \cong H_m \left( 2 / f \varkappa \right)^{1/2}$$

where $H_m$ is the mixed layer depth (Holton, 1972). Choosing representative values for the Arctic Ocean of $H_m$ = 40 m, $f$ = 1.4 X $10^{-4}s^{-1}$ and $\varkappa$ = 7 X $10^{-3}m^2s^{-1}$, we find a rapid response time of $\tau_e$ = 16 hr.

Below the mixed layer the strong stratification will suppress secondary circulation so that momentum and vorticity will be lost upward only by vertical eddy diffusion. Then the time scale will be

$$\tau_d \cong H_D^2 / \varkappa$$

17

where $H_D$ is taken as the distance from the base of the mixed layer to the subsurface velocity peak, about 100 m, and $\nu$ must have a reduced value of, say, $10^{-4} m^2/s$ so that

$$\tau_d \cong 3 \text{ yrs}$$

Thus the response time of the mixed layer at the surface is negligibly small in comparison with that of the stratified layers below it. We may then assume that the frictional effect of the ice is transmitted directly to the base of the mixed layer.

We examine the case of an initial vorticity profile with a maximum at the top, that is at the base of the mixed layer, where the vorticity remains zero due to friction and trace the changes in the profile with time as a subsurface maximum develops which resembles the observations. Since the horizontal and vertical structures are separable and since vertical vorticity is a horizontal derivative of velocity, the vertical profile derived for vorticity will also apply to velocity.

In the absence of vertical stretching and horizontal divergence, the linearized equation for vertical vorticity is a diffusion equation,

$$\frac{\partial^2 \zeta}{\partial z'^2} - \frac{1}{\nu} \frac{\partial \zeta}{\partial t} = 0$$

(4.1)

where vorticity

$$\zeta = \frac{\partial v}{\partial x} - \frac{\partial u}{\partial y}$$

In terms of a Fourier integral, (4.1) has a solution

$$\zeta(z,t) = \frac{1}{2(\pi\mu t)^{1/2}} \int_{-\infty}^{\infty} f(z') \, e^{-(z-z')^2/4\mu t} \, dz'$$

(4.2)

where the initial vorticity is f(z'). The boundary conditions are

$$\zeta = 0 \qquad at \qquad z = 0 \qquad for \quad t > 0$$

and

$$\zeta \rightarrow 0 \qquad as \qquad z \rightarrow -\infty \quad for \quad all \quad t \,.$$

Although the vertical profile derived from the previous baroclinic instability problem has the form of a modified Bessel function, we approximate that shape here with an exponential. Assume an exponential profile which has a mirror image above to maintain zero vorticity at z = 0.

$$f(z') = A \, e^{-az'} \qquad for \quad z > 0$$
$$= -A e^{az'} \qquad for \quad z < 0$$

Substituting into (4.2)

$$\zeta(z,t) = \frac{A}{2(\pi\mu t)^{1/2}} \left[ -\int_{-\infty}^{0} e^{az' - (z-z')^2/4\mu t} \, dz' \right.$$

$$\left. + \int_{0}^{\infty} e^{-az' - (z-z')^2/4\mu t} \, dz' \right]$$

19

or $\quad \zeta(z,t) = \dfrac{A}{2(\pi \mu t)^{1/2}} \left[ -e^{az + \mu t a^2} \displaystyle\int_{-\infty}^{0} e^{-[z' - (z + 2\mu t a)]^2 / 4\mu t} \, dz \right.$

$\left. + e^{-az + \mu t a^2} \displaystyle\int_{0}^{\infty} e^{-[z' - (z - 2\mu t a)]^2 / 4\mu t} \, dz' \right]$

$$(4.3)$$

In the first integral of (4.3), let

$$\frac{z' - (z + 2\mu t a)}{2(\mu t)^{1/2}} = \theta$$

and in the second integral, let

$$\frac{z' - (z - 2\mu t a)}{2(\mu t)^{1/2}} = \theta$$

This gives

$$\zeta(z,t) = A\pi^{-1/2} \left[ -e^{az + \mu t a^2} \int_{-\infty}^{-\frac{z + 2\mu t a}{2(\mu t)^{1/2}}} e^{-\theta^2} \, d\theta \right.$$

$$\left. + e^{-az + \mu t a^2} \int_{\frac{2\mu t a - z}{2(\mu t)^{1/2}}}^{\infty} e^{-\theta^2} \, d\theta \right]$$

20

Introducing the error function notation,

$$\operatorname{erf} \xi = 2\pi^{-1/2} \int_0^\xi e^{-\theta^2} d\theta$$

we have

$$\zeta(z,t) = A/2 \left\{ -e^{az + \nu t a^2} \left[ 1 + \operatorname{erf}\left( -\frac{z + 2\nu t a}{2(\nu t)^{1/2}} \right) \right] \right.$$
$$\left. + e^{-az + \nu t a^2} \left[ 1 - \operatorname{erf}\left( \frac{2\nu t a - z}{2(\nu t)^{1/2}} \right) \right] \right\}$$

(4.4)

Equation (4.4) may be evaluated in terms of normalized variables: for vorticity, $\zeta/A$ ; depth, az; and time, $a\,t^{1/2}$ (Fig. 11). Vorticity diffuses upward and downward so that a subsurface maximum develops which both decreases with time and descends to deeper levels. These theoretical profiles closely resemble the observed profiles, for example see Fig. 1.

From the previous results on baroclinic instability we may assume that $1/a$ = 200 m. The choice of an eddy coefficient is more difficult but experience in steep density gradients of other oceans suggests a value of $\nu$ = $10^{-4} m^2/s$ for an order of magnitude calculation. In the Arctic Ocean the velocity maximum occurs at 100 to 150 m. The mixed layer depth of 50 m must be subtracted to correspond to the theoretical problem. Then az = 0.25 to 0.5.

Referring to Fig. 11 it is seen that this corresponds to a dimensional decay time ranging from 46 to 185 days, indicating that the observed eddies had spent from 1 to 6 months beneath the ice. The decay time is directly proportional to choice of the eddy coefficient value which is admittedly a poorly known quantity and this eddy age can only be considered suggestive.

## 5. Summary and discussion.

The vigorous mesoscale features which are so abundant in the Arctic Ocean require a source of energy for their generation and maintenance. Although wind energy has been suggested as a source, the lack of correlation between winds and mesoscale motion makes this an unlikely relationship. Furthermore the arctic eddies are much smaller in horizontal scale than synoptic weather systems although a similar size might be expected if the eddies were driven by winds. Another possible energy source which has been suggested is thermodynamic in nature and associated with the freezing process. During winter, areas of open water appear in the ice pack through either breakup or differential motion of ice floes. Ice grows quickly in these open areas at the extremely low air temperatures which prevail. As the ice grows, salt is expelled and heavy brine sinks through the mixed layer causing intense local convection. But it is difficult to understand how this shallow convection can produce the observed redistribution of density at the much deeper levels where eddies are found. Also there is here again a mismatch in scales between the sizes of source and eddy. Open areas where rapid freezing occurs are usually tens to hundreds of meters across while the eddies are about 10 kilometers in

diameter. A more plausible source for eddy kinetic energy than either of these suggestions is the available potential energy residing in the inclined density surfaces accompanying the mean geostrophic circulation of the Arctic Ocean. The mean vertical shear has been shown to be unstable in the Barrow Current north of Alaska but not in the central Arctic Ocean where eddies were observed. The small-amplitude theory employed predicts an eddy size close to that observed and it predicts a growth rate fast enough to indicate rapid formation of these features. Although the theory cannot describe the evolution of an eddy, it is assumed that the unstable waves continue to develop until meanders form which eventually cut off to become isolated eddies.

The baroclinic instability theory used here applies to a vertical shear only and is appropriate to mid-ocean circulation where the horizontal shear may be considered negligible. It incorporates an exponential mean shear and stratification as well as Ekman pumping in an attempt to more closely fit actual oceanic conditions. The conclusion that the central Arctic Ocean is stable and that eddies do not originate there by this process seems quite definite. They must be formed elsewhere, apparently in the Barrow Current and application of the theory to this current confirms that it could be the source.

There are two assumptions inherent in the theory which are not exactly met in the Barrow Current however. The Current is a relatively narrow jet which has significant horizontal shear and it occurs along the shelf edge where the topography is not flat. But it is not believed that the conclusions reached would be seriously altered by inclusion of a horizontal mean shear effects and depth

variations. Although no quantitative modeling demonstrates this, some qualitative arguments make the omission of these effects appear relatively unimportant.

A mean horizontal shear may lead to instability and it is quite possible that the Barrow Current is barotropically as well as baroclinically unstable. The combined barotropic and baroclinic instability problem is an inseparable one and solutions to it have been primarily sought by numerical methods. Barotropic instability could only be expected to enhance eddy production. Its effect on growth rate and eddy size in this case will require further modeling in the future.

Bottom topography such as the continental margin in the vicinity of the Barrow Current is a departure from the level bottom assumed. Theoretical studies of topographic effects on the baroclinic instability problem cited in McWilliams (1979) review show that the classical Eady waves studied here are not strongly influenced by depth variations and that instability may even be enhanced by such variations. It is reasonable that bottom topography would not seriously modify the waves studied here which are trapped primarily against the upper surface of the ocean.

## ACKNOWLEDGEMENT

# REFERENCES

Charney, J. G., 1973. Planetary fluid dynamics in Dynamical Meteorology, edited by P. Morel, 99-351, D. Reidel Publ. Co., Dordrecht-Holland, 97-351.

Charney, J. and A. Eliassen, 1949. A numerical method for predicting perturbations in the middle latitude westerlies. Tellus, 1 (2), 38-54.

Eady, E. T., 1949. Long waves and cyclone waves. Tellus, 1 (3), 33-52.

Ekman, V. W., 1905. On the influence of the earth's rotation on ocean currents, Ark. f. Mat. Astr. och. Fysik, K. Sv. Vet. Ak., Stockholm, 1905-06, 2, 52 pp.

Gill, A. E., J. S. A. Green and A. J. Simmons, 1974. Energy partition in the large-scale ocean circulation and the production of mid-ocean eddies. Deep-Sea Res., 21, 499-528.

Green, J. S. A., 1960. A problem in baroclinic instability. Quart. J. R. Met. Soc., 86, 237-251.

Hart, J. E. and P. D. Killworth, 1976. On open ocean baroclinic instability in the Arctic, Deep-Sea Res., 23, 637-645.

Hunkins, K. L., 1974. Subsurface eddies in the Arctic Ocean. Deep-Sea Res., 21, 1017-1033.

Hunkins, K., 1980. Review of the AIDJEX oceanographic program, in Sea Ice Processes and Models, ed. by R. S. Pritchard, 33-45, Univ. of Wash. Press.

Kusunoki, K., 1962. Hydrography of the Arctic Ocean with special reference to the Beaufort Sea. Contr. Instit. Low Temp. Sci. Ser. A. No. 17, Hokkaido Univ., Sapporo, Japan, 74 pp.

Manley, T., 1981. Eddies of the western Arctic Ocean: their characteristics and importance to the energy,heat and salt balance. Doctoral dissertation, Columbia Univ., Unpubl. ms., 212 pp.

McWilliams, J., 1979. A review of research on mesoscale ocean currents, Rev. of Geophys. and Space Physics, 17(7), 1548-1558.

Newton, J. L., 1977. Oceanographic observations in the Northwest Greenland Sea--April 1977: Preliminary observations, Unpubl. ms.

Newton, J. L., K. Aagaard and L. K. Coachman, 1974. Baroclinic eddies in the Arctic Ocean. Deep-Sea Res., 21, 707-719.

Orlanski, I. and M. D. Cox, 1973.  Baroclinic instability in
    ocean currents.  Geophys. Fluid Dynam., 4, 297-332.

Pedlosky, J., 1979.  Geophysical Fluid Dynamics, Chap. 6, Springer-
    Verlag, New York, 624 pp.

Williams, G. P., 1974.  Generalized Eady waves.  J. Fluid Mech.,
    62, 643-655.

U. S. Naval Oceanographic Office, Oceanographic Data Report, Arctic,
    1959, Wash., D. C., Oct. 1963.  (Unpubl. ms.)

ILLUSTRATIONS

Fig. 1 - Profile of horizontal current through an Arctic Ocean eddy. Solid line is current speed and dashed line is direction, 5 May 1975, $76^\circ 23'N$ $149^\circ 48'W$ (Manley, 1981).

Fig. 2 - Profile of temperature (T), salinity (S), and density ($\sigma_t$) for the same eddy shown in Fig. 1. Solid lines are for conditions outside eddy in surrounding waters and dashed lines are for conditions inside eddy (Manley, 1981).

Fig. 3 - Locations of arctic eddies observed during drift of four AIDJEX ice camps. Of the 98 eddies for which rotation sense was determinable, 95 were anticyclonic or clockwise. The three cyclonic eddies are circled.

Fig. 4 - Phase speed and growth rate of baroclinic waves. $\hat{H} = 5$. Solid line is for rigid upper and lower surfaces with no friction. Dashed line is for Ekman pumping at a free upper surface and rigid lower surface, $W = 0.05$, $Y = 0.5$. Dotted line is for Ekman pumping at upper and lower rigid surfaces, $Y = 1$.

Fig. 5 - Phase speed and growth rate of baroclinic waves. $\hat{H} = 10$. Symbols as in Fig. 4.

Fig. 6 - Relative amplitude, M, and negative phase, $-\theta$, of fastest-growing wave. Rigid upper and lower surfaces with no Ekman pumping. $\hat{H} = 5$ and $\hat{K} = 0.8$.

Fig. 7 - Relative amplitude, M, and negative phase, $-\theta$, of fastest-growing wave. Ekman pumping with free upper and rigid lower surface. $\hat{H} = 5$ and $\hat{K} = 0.7$.

Fig. 8 - Relative amplitude, M, and negative phase, $-\theta$, of fastest-growing wave. Ekman pumping with rigid upper and lower surfaces. $\hat{H} = 5$ and $\hat{K} = 0.4$.

Fig. 9 - Geostrophic currents in the Arctic Ocean. Profiles (1) and (2) are in the central Arctic Ocean, (3) is near the shelf edge north of Alaska (Kusunoki, 1962).

Fig. 10 - Profiles of Väisälä frequency in the central Arctic Ocean.

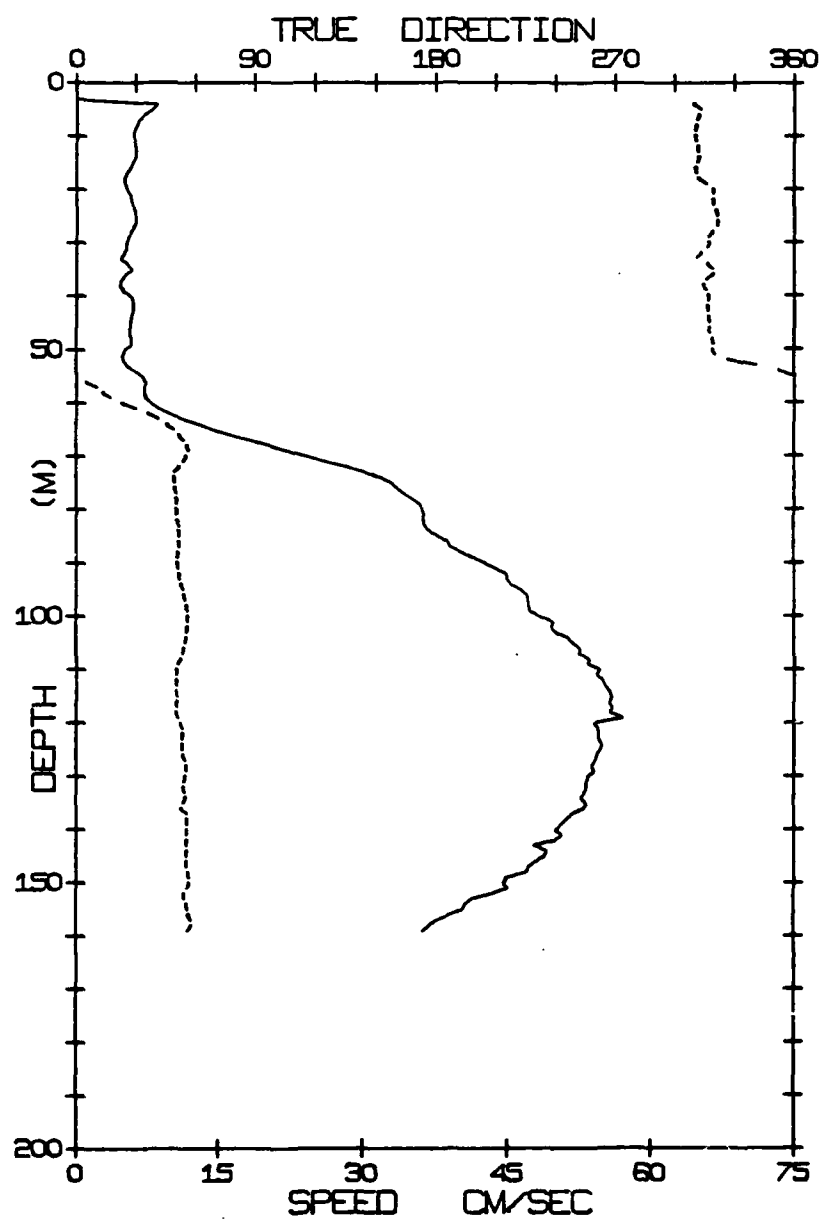Fig. 11 - Development of a vorticity profile with a subsurface maximum from an initial exponential profile. Vorticity at the upper surface is kept at zero by frictional dissipation.
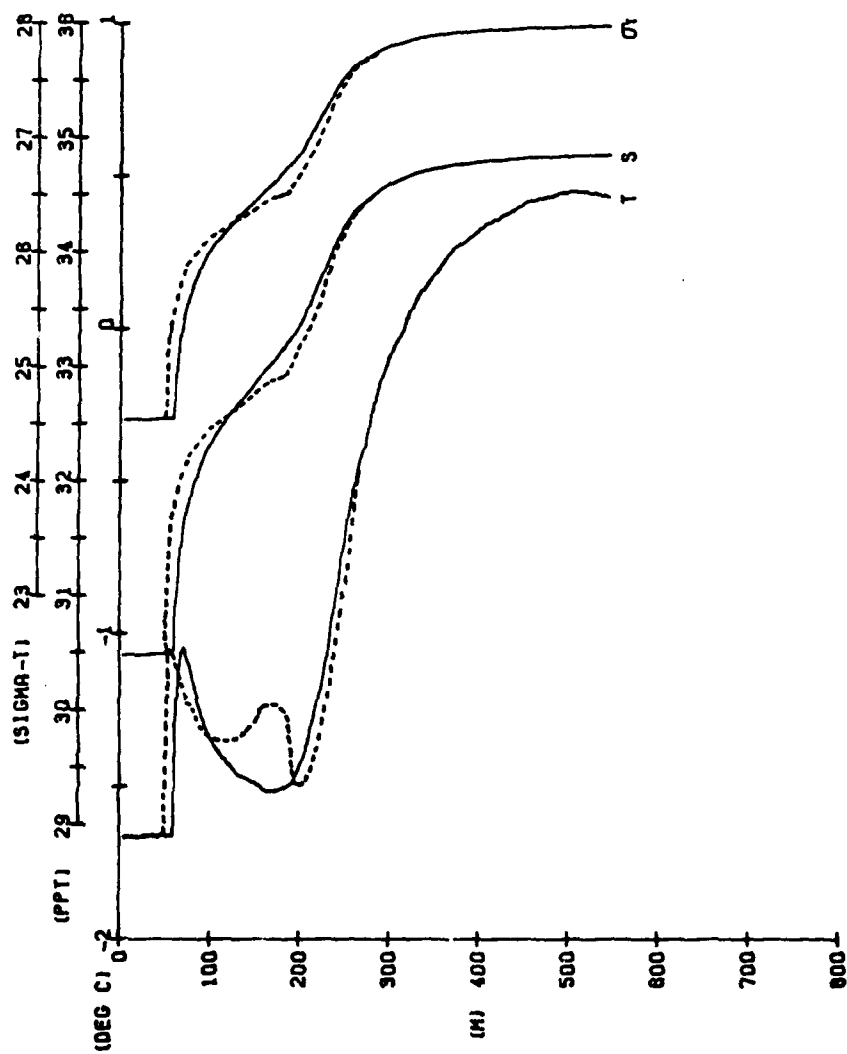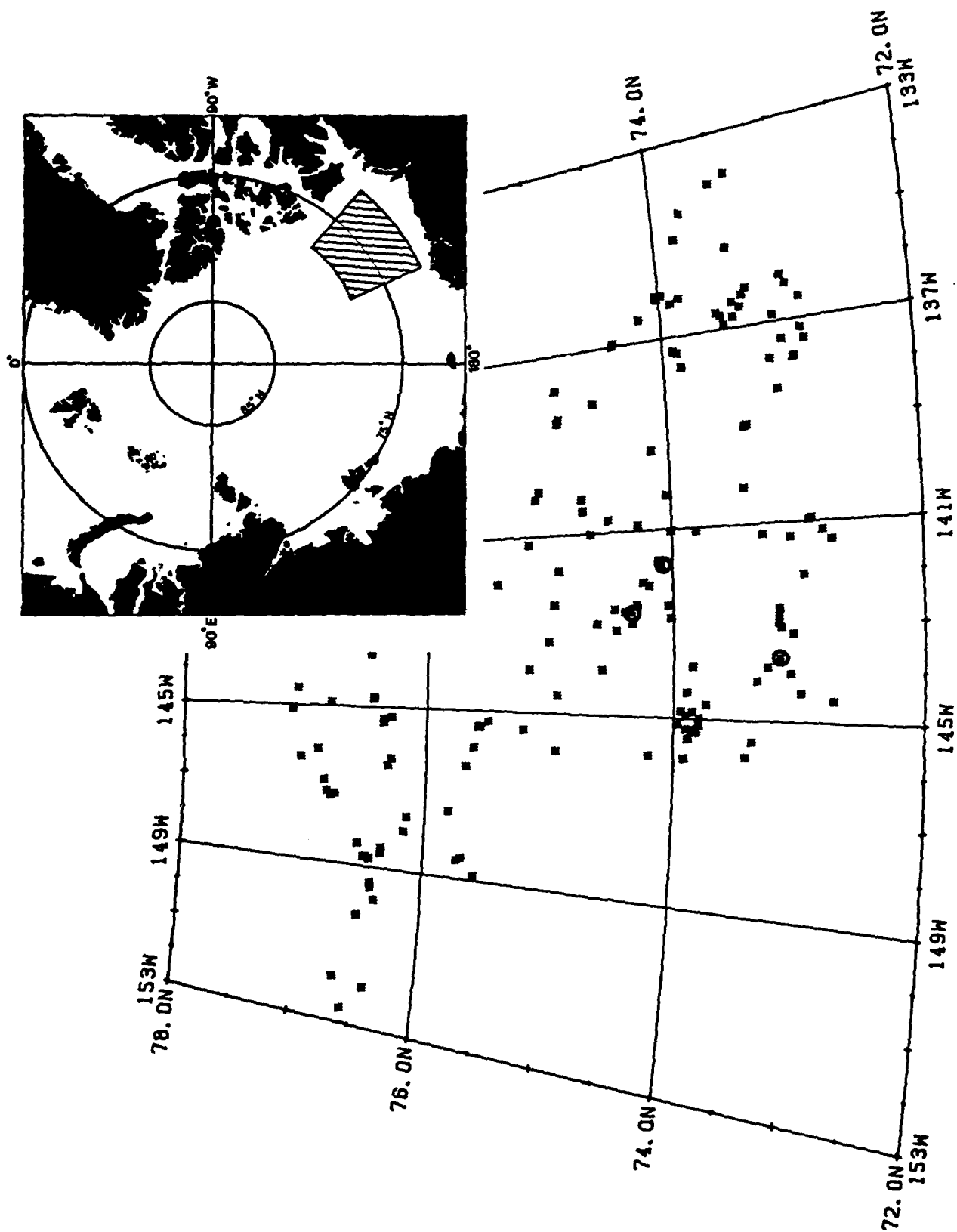
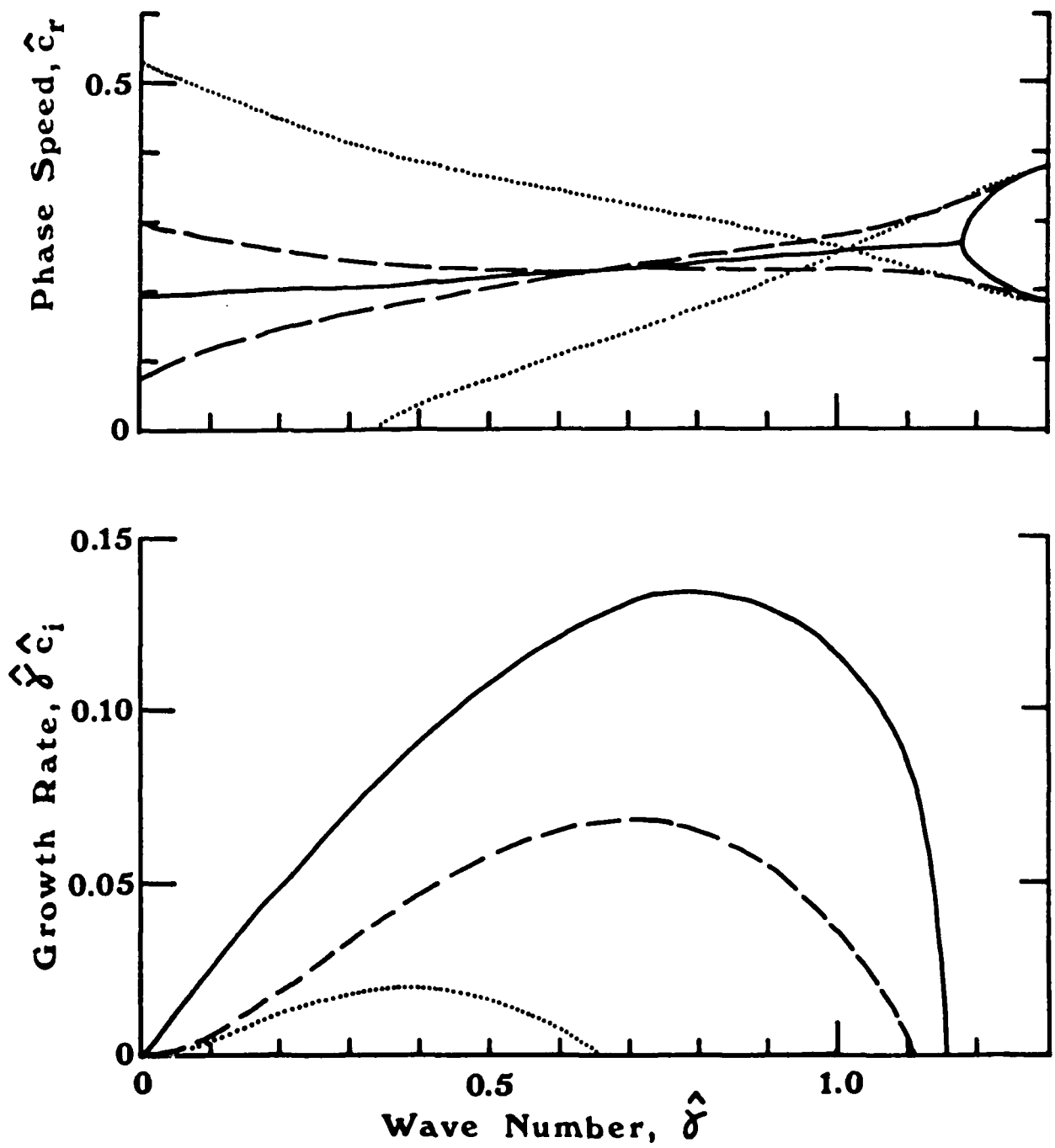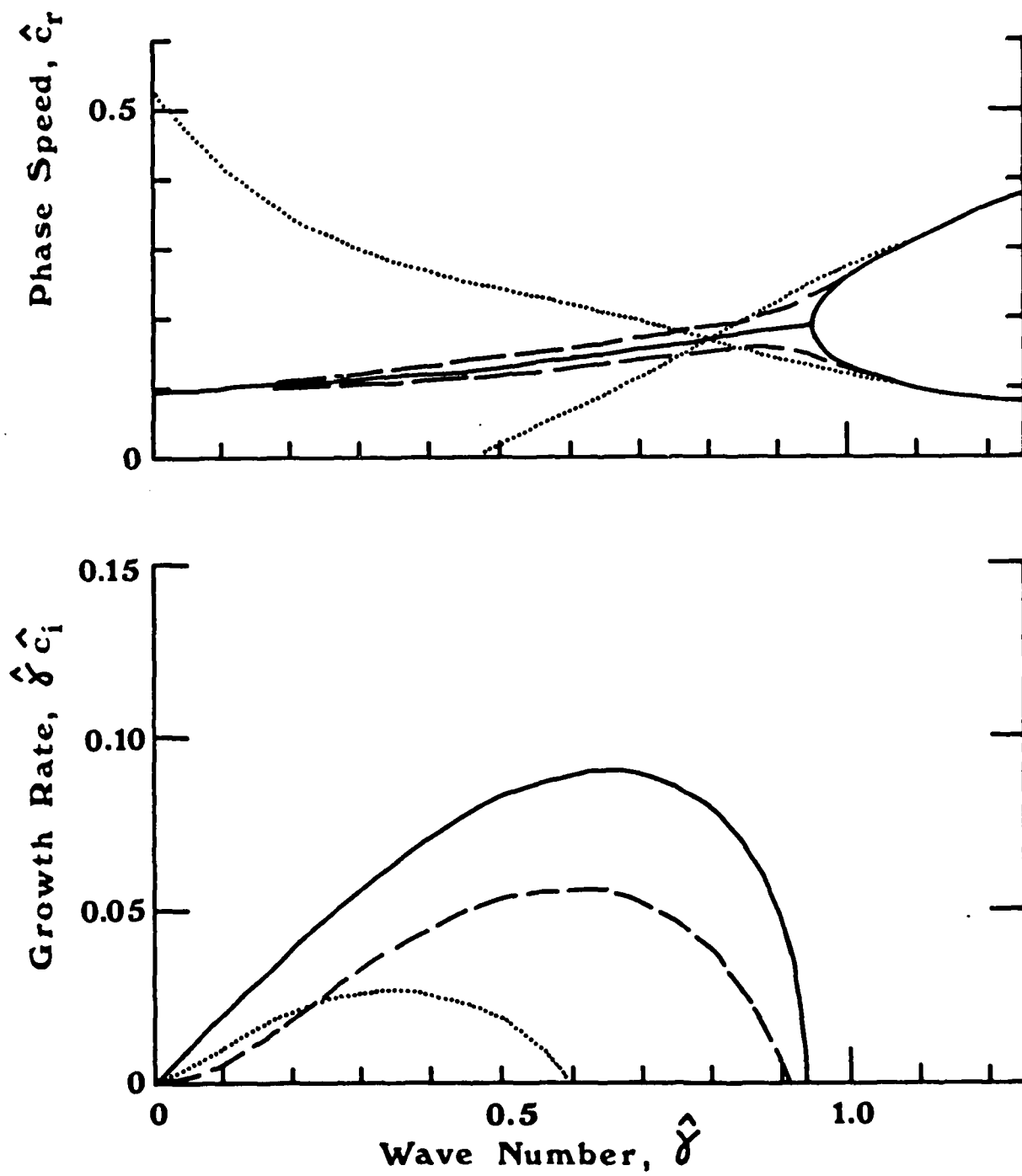Fig. 1

Fig. 2

Fig. 3

Fig. 4

Fig. 5

Fig. 6

34
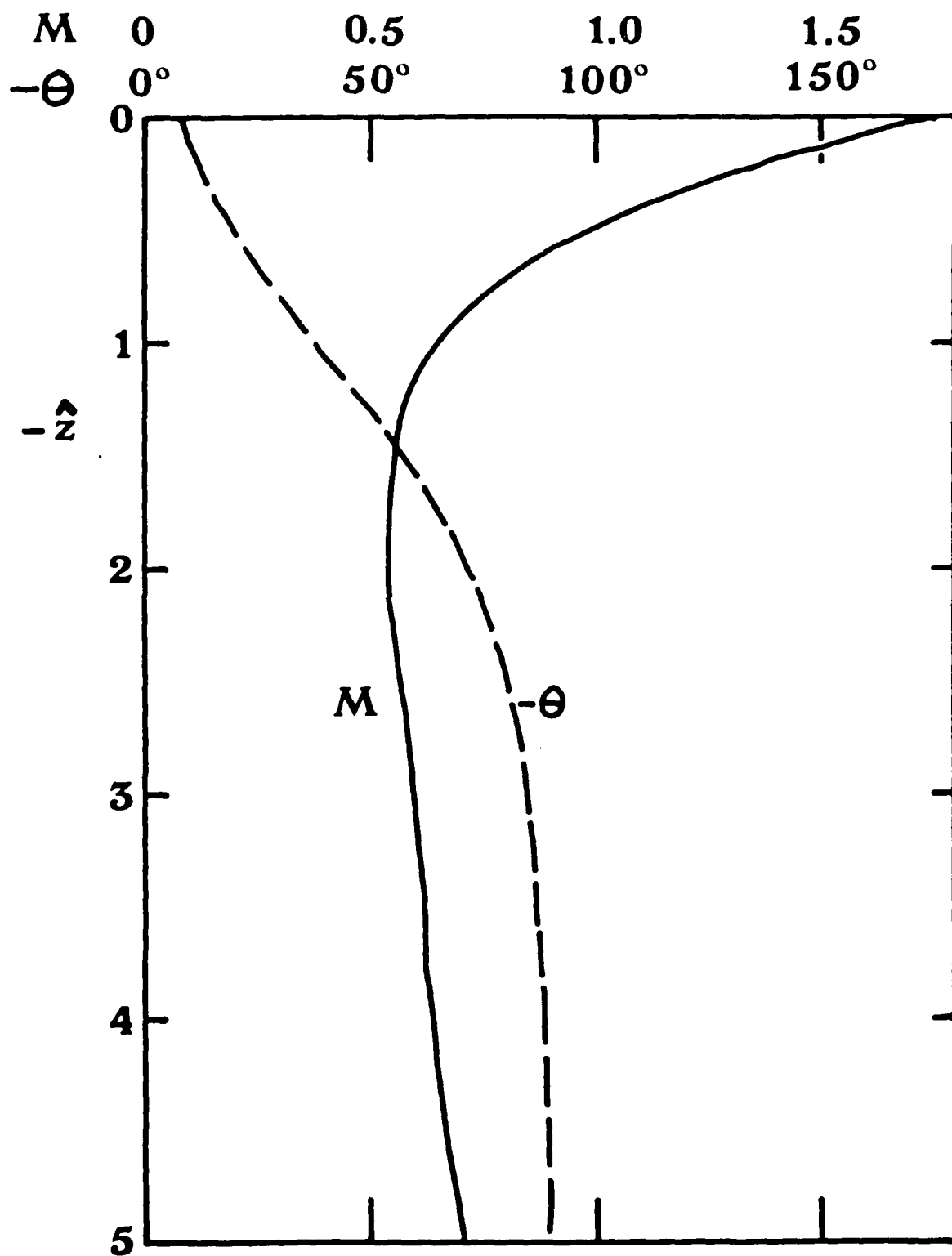
Fig. 7

Fig. 8

Fig. 9



CURRENT VELOCITY, cm/sec

Fig. 10

38

FIG. 11



RELATIVE VORTICITY, $\zeta/A$

DEPTH, $az$
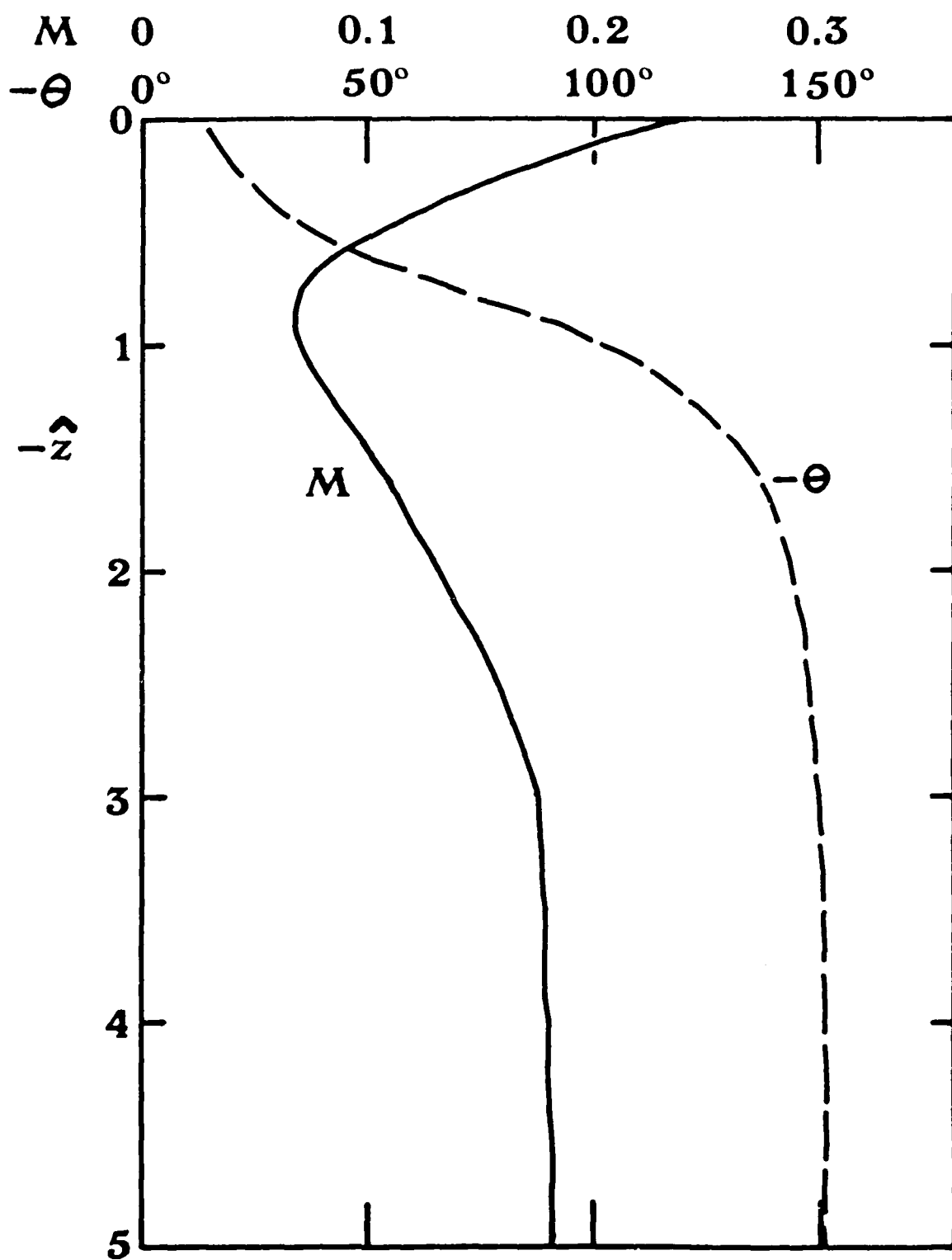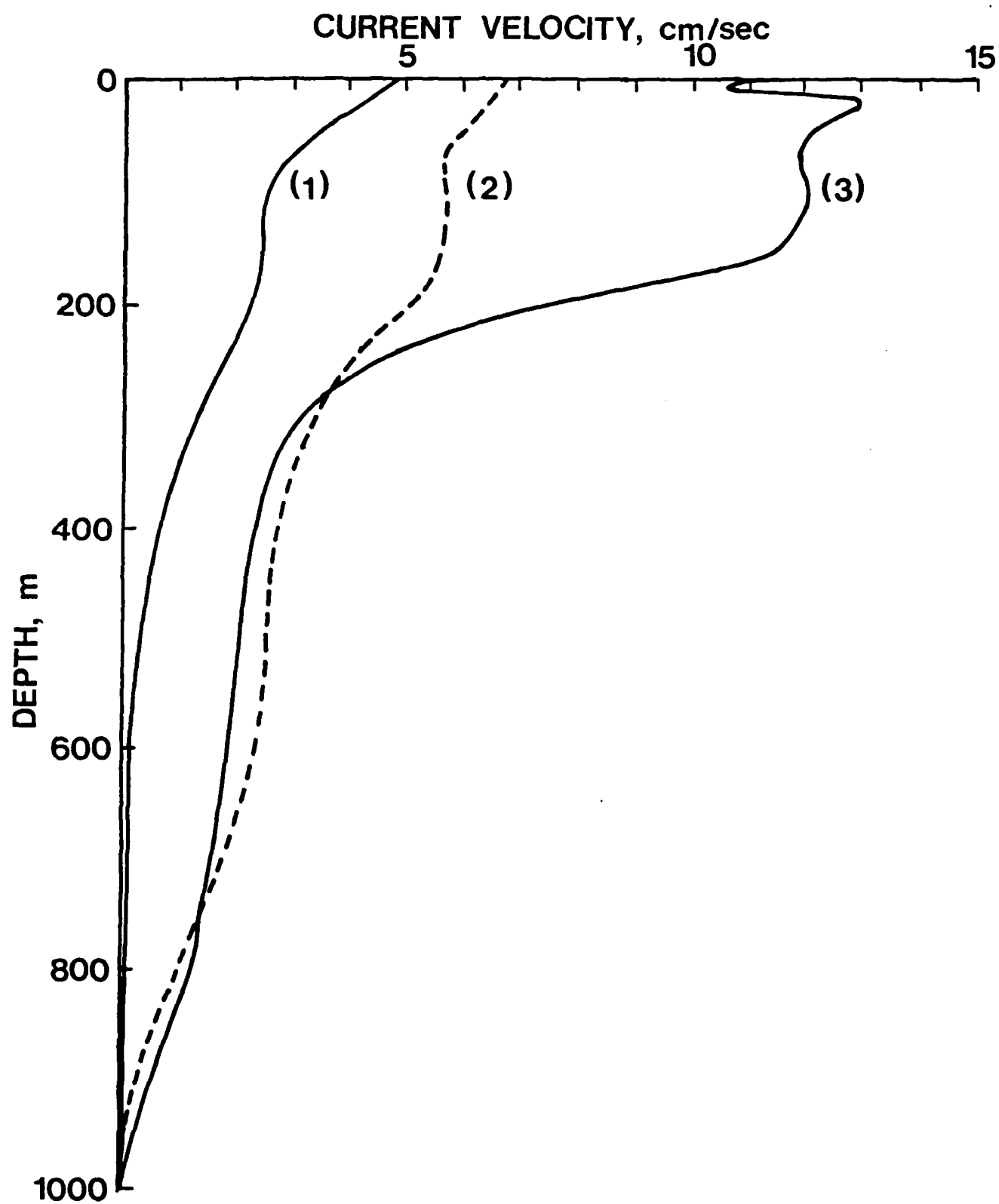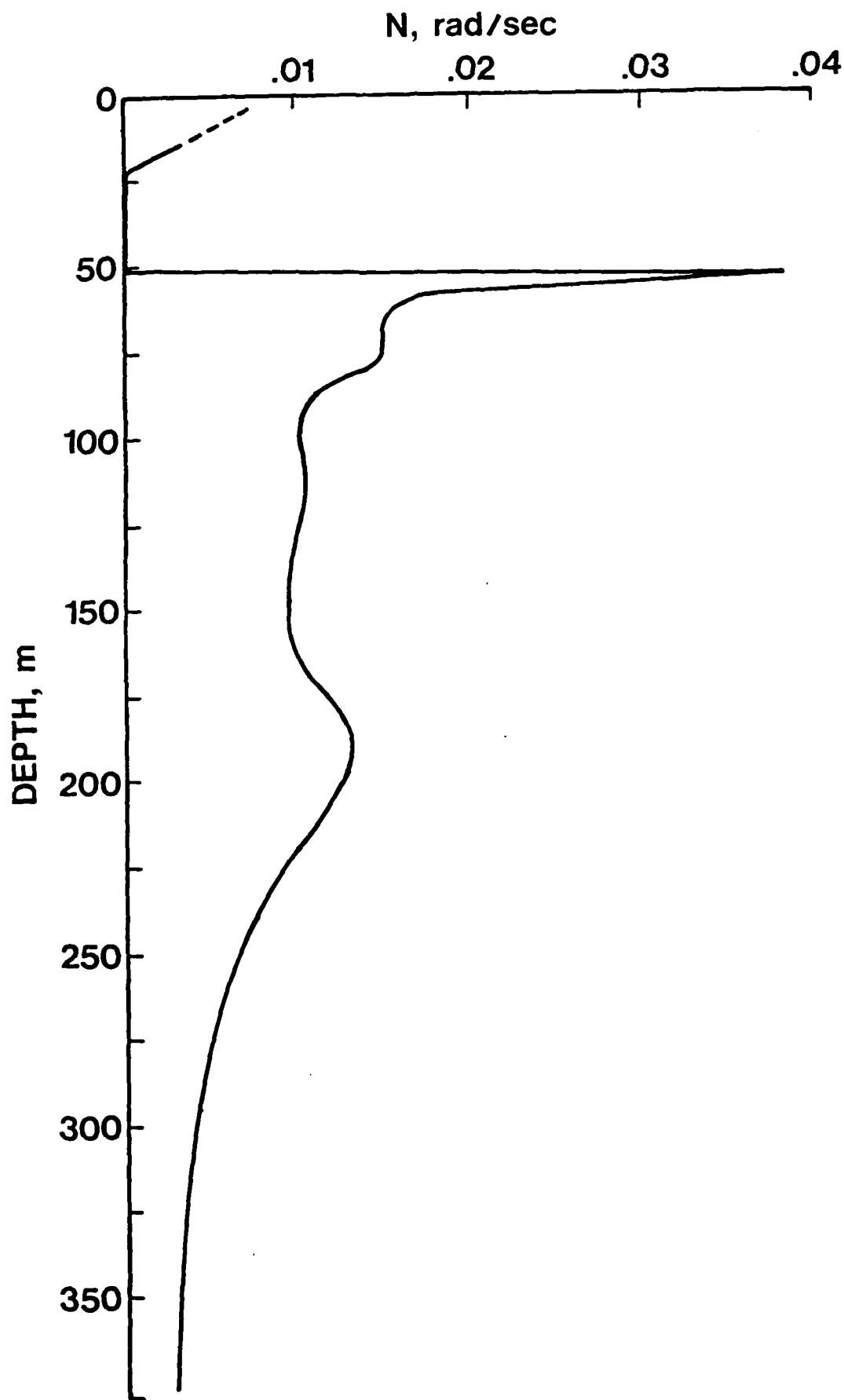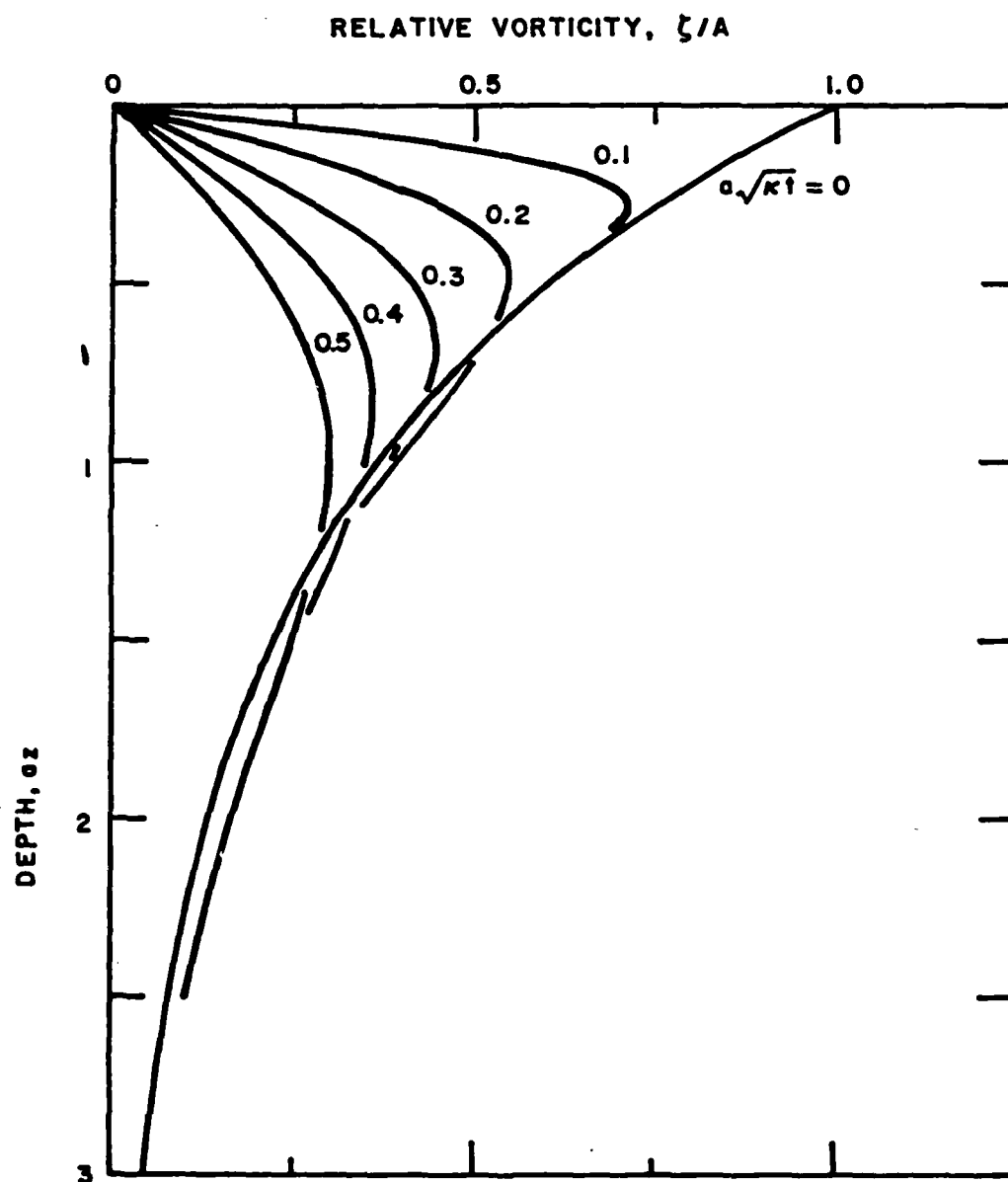
MANDATORY
DISTRIBUTION LIST


FOR UNCLASSIFIED TECHNICAL REPORTS, REPRINTS, & FINAL REPORTS
PUBLISHED BY OCEANOGRAPHIC CONTRACTORS
OF THE OCEAN SCIENCE AND TECHNOLOGY DIVISION
OF THE OFFICE OF NAVAL RESEARCH


1  Director of Defense Research and
     Engineering
   Office of the Secretary of Defense
   Washington, D. C. 20301
   ATTN:  Office, Assistant Director
               (Research)


   Office of Naval Research
   Arlington, VA 22217
1  ATTN:   (Code 102-C)
1  ATTN:   (Code 200)
1  ATTN:   (Code 460)
3  ATTN:   (Code 480)


6  Director
   Naval Research Laboratory
   Washington, D. C. 20375
   ATTN:  Library, Code 2620


1  U. S. Naval Research Laboratory
   Code 2627
   Washington, D. C. 20375


2  Office of Naval Research - N.Y.
   715 Broadway
   New York, N. Y. 10003


12 Defense Documentation Center
   Cameron Station
   Alexandria, VA 22314


1  Commander
   Naval Oceanographic Office
   NSTL Station
   Bay St. Louis, MS 39522
   ATTN:  Code 02

| REPORT DOCUMENTATION PAGE | | READ INSTRUCTIONS BEFORE COMPLETING FORM |
|---|---|---|
| 1. REPORT NUMBER LDGO-CU-2-81 | 2. GOVT ACCESSION NO. AD-A101 620 | 3. RECIPIENT'S CATALOG NUMBER |
| 4. TITLE (and Subtitle) ARCTIC OCEAN EDDIES AND BAROCLINIC INSTABILITY | | 5. TYPE OF REPORT & PERIOD COVERED Technical Report March 1981 to May 1981 |
| | | 6. PERFORMING ORG. REPORT NUMBER |
| 7. AUTHOR(s) Kenneth Hunkins | | 8. CONTRACT OR GRANT NUMBER(s) N00014-76-C-0004 |
| 9. PERFORMING ORGANIZATION NAME AND ADDRESS Lamont-Doherty Geological Observatory of Columbia University Palisades, N. Y. 10964 | | 10. PROGRAM ELEMENT, PROJECT, TASK AREA & WORK UNIT NUMBERS NR307-359 |
| 11. CONTROLLING OFFICE NAME AND ADDRESS Dept. of Navy, Office of Naval Research Code 461, Arlington, VA. 22217 | | 12. REPORT DATE July 1981 |
| | | 13. NUMBER OF PAGES 39 |
| 14. MONITORING AGENCY NAME & ADDRESS(if different from Controlling Office) Same As Above | | 15. SECURITY CLASS. (of this report) Unclassified |
| | | 15a. DECLASSIFICATION/DOWNGRADING SCHEDULE |

16. DISTRIBUTION STATEMENT (of this Report)

Approved for public release; distribution unlimited
Reproduction in whole or in part is permitted for any purpose
of the United States Government.

17. DISTRIBUTION STATEMENT (of the abstract entered in Block 20, if different from Report)

18. SUPPLEMENTARY NOTES

19. KEY WORDS (Continue on reverse side if necessary and identify by block number)

Eddies, Arctic Ocean, baroclinic instability,
mesoscale variability

20. ABSTRACT (Continue on reverse side if necessary and identify by block number)

Baroclinic eddies with diameters of about 10 km and maximum
current speeds of about 50 cm/s have beeb widely observed in the
central Arctic Ocean north of Alaska and Canada. The possible
origin of these eddies through an instability of th mean baro-
clinic flow is investigated using an model with exponential
profiles of mean shear and Väisälä frequency. The model includes
Ekman pumping at a rigid bottom and at either a free or rigid

DD FORM 1473 EDITION OF 1 NOV 65 IS OBSOLETE
1 JAN 73
S/N 0102-LF-014-6601

upper surface. The central Arctic Ocean where the eddies were
found is baroclinically stable with no possibility of eddy pro-
duction. If eddies are spawned by this mechanism, they must
be formed at a site far from where they are observed. On the
periphery of the Arctic Ocean north of Alaska the combination of
greater current shear, shallower depth and lack of ice cover
leads to unstable conditions and the eddies apparently originate
in that region. The instability theory predicts maximum velocity
at the surface instead of below the surface as observed. Appar-
ently after formation in the open water the eddies are advected
beneath the ice cover and dissipate the momentum of their upper
layers against the ice. This is demonstrated by calculations for
the diffusion of vorticity against the ice in the case of an
initial exponential profile. A subsurface maximum then develops
which resembles the observed profiles.